Energy and charge transfer in blends of dendronized perylenes with polyfluorene

Jaiser, Frank; Neher, Dieter; Meisel, Andreas; Nothofer, Heinz-Georg; Miteva, Tzenka; Herrmann, Andreas; Müllen, Klaus; Scherf, Ullrich

Published in:
The Journal of Chemical Physics

DOI:
10.1063/1.2976769

Publication date:
2008

Energy and charge transfer in blends of dendronized perylenes with polyfluorene

Frank Jaiser,[1] Dieter Neher,[1,a)] Andreas Meisel,[2,b)] Heinz-Georg Nothofer,[2,c)] Tzenka Miteva,[2,c)] Andreas Herrmann,[2,d)] Klaus Müllen, and Ullrich Scherf[3]
[1]*Institut für Physik und Astronomie, Universität Potsdam, Karl-Liebknecht-Str. 24-25, 14476 Potsdam-Golm, Germany*
[2]*Max-Planck-Institut für Polymerforschung, Ackermannweg 10, 55021 Mainz, Germany*
[3]*Makromolekulare Chemie, Bergische Universität Wuppertal, Gaußstraße 20, 42119 Wuppertal, Germany*

(Received 28 April 2008; accepted 7 August 2008; published online 15 September 2008)

Two generations of polyphenylene dendrimers with a perylene diimide core are compared with a nondendronized tetraphenoxyperylene diimide model compound regarding their application in organic light-emitting diodes (OLEDs). Single layer devices with blends of the first and second generation dendrimers in polyfluorene are investigated as active layers in OLEDs, and the effect of dendronization on the emission color and electroluminescence intensity is studied. In photoluminescence, higher degrees of dendronization lead to a reduction in Förster transfer from the polyfluorene host to the perylene, resulting in a larger contribution of the blue host emission in the photoluminescence spectra. In electroluminescence, the dopants appear to act as active traps for electrons, resulting in a predominant generation of excitons on the dye. This gives rise to a remarkably stronger contribution of red emission in electroluminescence than in photoluminescence where energy is exchanged exclusively via Förster transfer. The pronounced color change from red to blue with higher degrees of dendronization and larger driving voltages is explained by the competition of the recombination of free electrons with holes and trapping of electrons by the emitting guest. © *2008 American Institute of Physics*. [DOI: 10.1063/1.2976769]

INTRODUCTION

The design of organic light-emitting structures, which emit light at several regions of the visible spectrum, is a very active area of research on polymer-based organic electroluminescence (EL). Among the various concepts developed for the emission of light in a broad wavelength range,[1–5] the host-guest approach, which comprises a blue-emitting wide band-gap polymer host and one or several smaller band-gap emissive guests, is of greatest interest with regard to simplicity of device fabrication.[6–9] More recently, efficient emission from side-chain copolymers with blue-, green-, and red-emitting components has been demonstrated.[10–14] In multicomponent devices, the direct recombination of charges on the polymer host competes with the transfer of excitation to the guest, which can have three different origins: (a) Förster transfer of singlet excitons generated on the host to the guest, (b) Dexter transfer of triplet excitons generated on the host to the guest (in the case of phosphorescent dopants), and (c) direct generation of singlet and triplet excitons on the guest by sequential trapping of charges. Color-stable emission requires a careful balance of the kinetics of these processes.

The decoration of emitters with dendronic side groups ("dendronization") offers the possibility to control the degree of intermolecular interactions and thus the kinetics and efficiency of energy and charge transfer processes.[15–22] In 2004, we published a detailed study on a blend consisting of a dendronized perylene diimide (PDI) emitter, the hole-transporting polymer poly(*N*-vinylcarbazole) PVK, and the electron-transporting nonpolymeric compound 2-(4-biphenylyl)-5-(4-tert-butylphenyl)-1,3,4-oxadiazole (PBD).[23] PDI derivatives have been successfully used as functional dyes in fluorescent solar collectors,[24] photovoltaic cells,[25] optical switches,[26] lasers,[27] and light-emitting diodes[28–30] because of their excellent chemical, thermal, and photochemical stability.[31] In this earlier study, the PDI-luminophore was shielded with polyphenylene dendrons consisting of tetraphenyl-substituted benzene repeat units attached at the bay positions of the PDI chromophore (Chart 1). To improve solubility, the polyphenylene dendrons had been additionally equipped with bulky alkyl substituents. The PVK:PBD host was chosen because of its very good function in highly efficient electrophosphorescent diodes.[32–35]

In the blend of the dendritic dyes with the PVK:PBD matrix, we observed a significant reduction in guest emission in both PL and EL with increasing generation number, indicating that the dendritic shell reduces the efficiency of both energy and charge transfer to the emissive core. To explain these effects in a more quantitative fashion, we developed a model taking into account both Förster transfer of excitons as well as transfer of electrons from the host to the guest. Surprisingly, the effect of dendron size on the rate of electron

[a)]Author to whom correspondence should be addressed. Electronic mail: neher@uni-potsdam.de.
[b)]Present address: Innovalight Inc., 3303 Octavius Drive, Santa Clara, CA 95054, USA.
[c)]Present address: Sony Deutschland GmbH, Materials Science Laboratory, Hedelfinger Straße 61, 70327 Stuttgart, Germany.
[d)]Present address: Zernike Institute for Advanced Materials, Department of Polymer Chemistry, Nijenborgh 4, 9747 AG Groningen, The Netherlands.

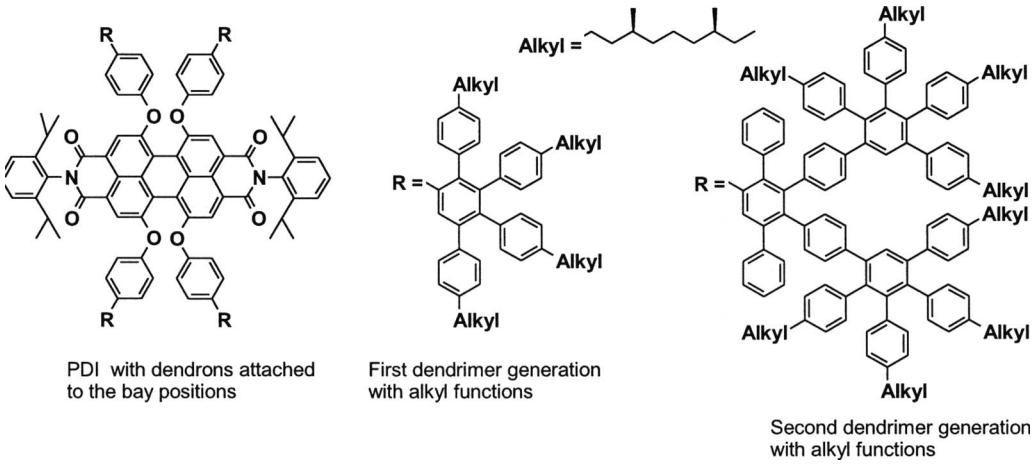

CHART 1. Structure of PDI dendrimers with dendrons attached to the bay positions of the chromophore that were employed in a former study (Ref. 23).

capture by the dendronized dye was quite weak. From the experimentally determined intensity ratios, we concluded that the trapping coefficient decreases by a factor of only about 3 for each additional dendritic shell (generation). This factor appears small when considering the significant change in the thickness of the shell with increasing generation. One possible explanation for this effect is that the low molecular weight PBD might penetrate into the dendritic scaffold, leading to a reduced distance for electron transfer to the emissive core. In addition, the flexible alkyl chains in the periphery of the dendrimers might largely affect the morphology of the blend and thus the transfer rates. The excited state on the PVK:PBD host was shown to be an intermolecular exciplex rather than an intramolecular exciton.[36,37] It can be expected that the presence of long and bulky alkyl substituents at the periphery of the dendrimers alters the efficiency for the formation of exciplexes on the PVK:PBD host.

Here, we present studies on the energy and charge transfer in a blend of triphenylamine-end-capped polyfluorene (TPA-PF) with structurally different PDI dendrimers, having the polyphenylene dendrons now attached to the imide moiety of the PDI core (Chart 2). The dense packing of the benzene rings and the inherent stiffness of the phenyl-phenyl-bonds in the dendrons provide a shape-persistent dendritic shell of high thermal and chemical stability.

Subject to this study are the polyphenylene dendrimers of the first (G1) and second (G2) generations as well as a nondendronized tetraphenoxyperylene diimide model compound (M) (Chart 2). The polyfluorene TPA-PF (Chart 3) and related polyfluorenes have been extensively used as emitter in blue-emitting organic light-emitting diodes (OLEDs)[38–41] as well as host for emissive guests in red and white light-emitting diodes.[8,42–47] The primary excited state of polyfluorenes is an intrachain exciton rather than an intermolecular species. An interpenetration of the polyfluorene backbone and the dendritic shell is rather unlikely, which simplifies the interpretation of energy transfer processes. Based on these components, two different kinds of LEDs have been investigated. In a first approach, the active layers of the devices consist of the pure materials M, G1, and G2 to demonstrate the reduction in aggregation for the dendritic structures. Next, these materials were doped as guest molecules into TPA-PF to investigate the charge transport and energy transfer in this system.

EXPERIMENTAL SECTION

The synthesis of the ethynyl functionalized tetraphenoxy PDI core and the subsequent buildup of three generations of dendrons via repetitive Diels–Alder reactions with tetraphenylcyclopentadianone building blocks are described elsewhere.[17]

OLED and hole-only devices

For the fabrication of the devices, glass substrates patterned with 100 nm thick indium tin oxide (ITO) electrodes (Balzers) were cleaned subsequently in ultrasonic baths of acetone, ionic detergent water solution, ultrapure water (MilliQ unit from Waters), and isopropanol. After drying, a 20 nm thick layer of polyethylenedioxythiophene doped with poly(styrene sulfonate) (PEDT:PSS) was spin coated on top. The films were dried in vacuum for 6 h at room temperature. The emitting materials (the pure PDI chromophores or the dyes blended into TPA-PF) were spin coated on top, resulting in a final thickness of 80 nm. Pure M, G1, G2, and TPA-PF were spin coated from 10 mg/ml toluene solutions, and the blend solutions were prepared by adding the respective dye from a 3 mg/ml toluene solution to the solution of TPA-PF at concentrations of 3 wt %. All solutions were filtered immediately before spin coating through 0.45 μm filters. The solution preparation and layer deposition were done under ambient conditions. After drying overnight under vacuum at room temperature, an approximately 1 nm thick LiF electron injection layer was deposited by thermal evaporation at a pressure of $\approx 6 \times 10^{-6}$ mbar at a rate of 1 Å/s. Subsequently, the top electrode consisting of 20 nm Ca and a 100 nm thick protective Al layer was evaporated at a rate of 7 Å/s for Ca and 5 Å/s Al. The overlap between the bottom and top electrodes resulted in a device area of 5 mm^2. Hole-only devices were single layer devices with films of TPA-PF blended with the respective dyes (the resulting layer thickness was 80 nm) sandwiched between ITO and a 50 nm

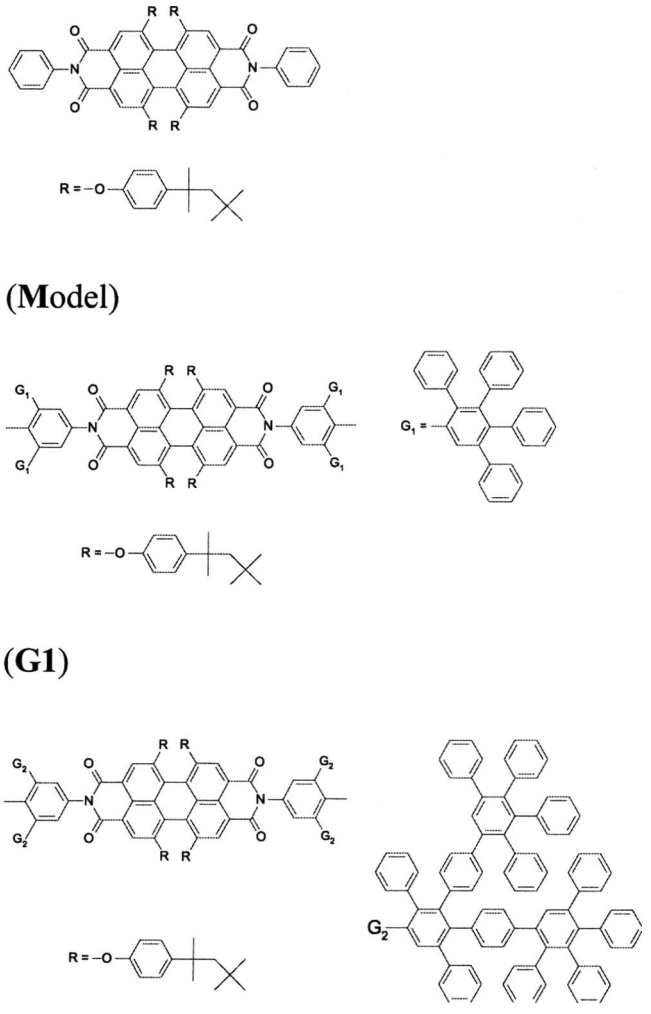

CHART 2. Structure of the nondendronized tetraphenoxyperylene diimide model compound (M) and the polyphenylene dendrimers of the first (G1) and second (G2) generations used in this study.

thick gold top electrode, evaporated at a rate of 1 Å/s. The device characterization was carried out in an evacuated sample chamber. The Commission Internationale de l'Eclairage 1931 (CIE 1931) color coordinates of the emission in photoluminescence (PL) were calculated from the respective PL spectra shown in Fig. 2 by using CIE color matching functions.[48,49] The EL color coordinates were measured with a Minolta ChromaMeter CS-100.

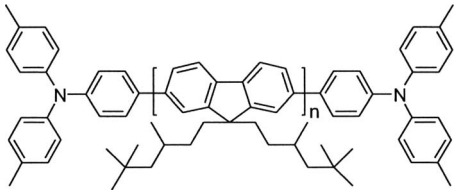

CHART 3. Structure of α,ω-bis[*N*,*N*-di(4-methylphenyl)aminophenyl]-poly(9,9-bis(3,5,5-trimethylhexyl)fluorene-2,7-diyl) (TPA-PF).

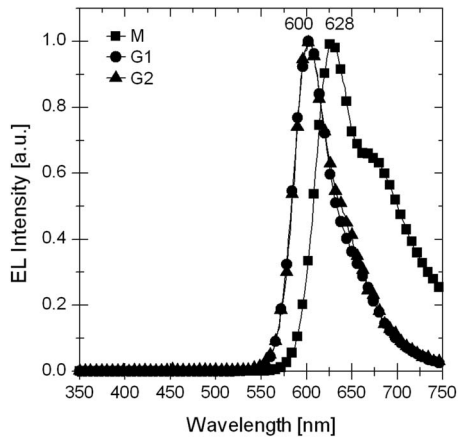

FIG. 1. EL spectra of ITO/PEDOT/dendrimer/Ca/Al single layer devices with M (squares), G1 (circles), and G2 (triangles) as pure layers.

RESULTS AND DISCUSSION

LEDs based on pure model compound and dendrimers

Figure 1 contains the EL spectra of the devices with pure M, G1, and G2. The spectra of the dendronized and nondendronized model materials differed substantially from each other, whereas the spectra of G1 and G2 were almost identical. The characteristics of the spectrum of M, a 95 nm full width at half maximum and its additional shoulder, clearly evidence aggregation due to closely packed chromophores.[50] Contrary, the blueshifted and narrow spectra of the dendrimers G1 and G2 indicate that the π-stacking was suppressed to the same degree in both generations.

The onset voltages of the devices with the pure materials as active layers were rather low with 4 V in the case of M and G1 and 7 V for G2. For single layer devices with the nondendronized compound M, the brightness was 11 cd/m^2 at 18 V only. Red EL with a luminance of 120 cd/m^2 at 11 V was obtained for pure G1 with CIE 1931 color coordinates (0.627, 0.372). For G2, the luminance was 13 cd/m^2 at 18 V, which we attribute in part to the isolating effect of the dendritic scaffold.[18] In all cases the films made of the pure dyes were noncontinuous, resulting in large leakage currents. Consequently, luminance efficiencies of these LEDs were quite low, with values of approximately 0.03 cd/A for the best devices.

Doping of M, G1, and G2 into TPA-PF

To investigate the influence of the degree of dendronization on the energy and electron transfer from a polymer host to the emissive core of dendronized guests, M, G1, and G2 were blended into TPA-PF. Comparable TPA-end-capped polyfluorenes with a slightly less bulky structure were shown to yield bright and efficient blue electroluminescence.[41] The polyfluorene derivative used here was chosen because it showed good compatibility with M, G1, and G2. The perylene-containing dopants M, G1, and G2 were blended at a concentration of 3 wt % into TPA-PF. Due to the higher molecular weights of the dendrimers, the number concentration of the active perylene chromophore was lower for G1

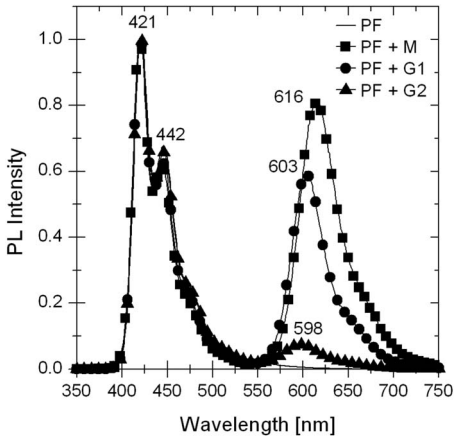

FIG. 2. PL spectra (normalized to the peak at 421 nm) of blends of TPA-PF and 3 wt % of M (squares), G1 (circles), and G2 (triangles). For comparison, the spectrum of the pure TPA-PF (no symbols) is also shown. The excitation wavelength was 340 nm.

and G2 than for M and was estimated to 1.3×10^{19}, 6.2×10^{18}, and 3.0×10^{18} cm^{-3} for M, G1, and G2, respectively.

Energy transfer in photoluminescence

Figure 2 shows the normalized PL spectra of films of pure TPA-PF and of blends with 3 wt % of the respective dyes M, G1, and G2. In all cases an excitation wavelength of 340 nm, close to the wavelength of minimum absorption of the dopant, was chosen to avoid any contribution from excitons generated directly on the perylene dye. As can be seen from the PL spectra, the dopant emission decreased in the series M, G1, and G2. Doping with the nondendronized M yielded the most efficient energy transfer from the TPA-PF host molecules. The peak in the longer wavelength region was located at 616 nm and reached 80% of the intensity of the strongest TPA-PF emission peak at 421 nm. From the spectra, color coordinates for PL emission of (0.39, 0.19) were calculated. For the dendrimer G1, the red peak was shifted to 603 nm and reached 60% of the TPA-PF peak height, yielding CIE values of (0.35, 0.18). For G2, the peak in the red was centered at 598 nm and was weak compared to the blue emission of the host. The corresponding color coordinates were (0.19, 0.08).

For singlet energy transfer, dipole-dipole Förster interaction is the dominating factor.[51,52] An important measure for a quantitative description of the probability of energy transfer is the Förster radius (R_0) of the respective guest-host system. This radius is equivalent to the donor-acceptor distance at which energy transfer is as probable as depopulation of the excited state via fluorescence, internal conversion, or intersystem crossing.

The PL emission spectrum of TPA-PF excited at 340 nm and the absorption spectra of M, G1, and G2 are shown in Fig. 3. It is evident that the PL spectrum of TPA-PF with its two maxima at 421 and 442 nm overlaps strongly with the short-wavelength absorption bands of M, G1, and G2, which are located at 450 and 443 nm, respectively. From these spectra the Förster radii (R_0) for the respective guest-host systems were calculated according to the relation[51,52]

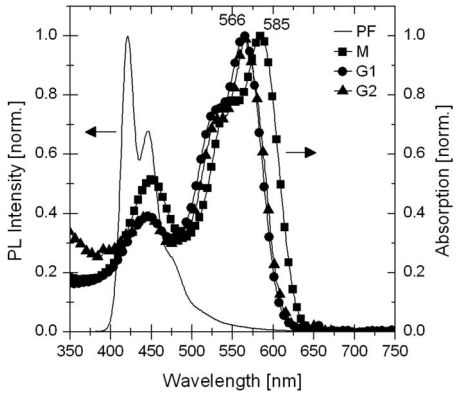

FIG. 3. Fluorescence spectra of pure TPA-PF (no symbols) and absorption spectra of M (squares), G1 (circles), and G2 (triangles). All spectra are normalized to their respective emission maxima.

$$R_0^6 = \frac{9000 \ln 10}{128\pi^5} \frac{\kappa^2 \phi_{\text{host}}}{N_A n^4} J, \tag{1}$$

where κ^2 is an orientation factor (2/3 for random orientations of donor and acceptor), ϕ_{host} is the fluorescence quantum yield of the donor in the absence of the acceptor (approximately 50% for polyfluorene), N_A is the Avogadro's constant, and n is the refractive index of the host system ($n_{\text{PF}}=2$). J is the mentioned overlap integral between the donor fluorescence spectrum and the acceptor absorption spectrum,

$$J = \int_0^\infty F_{\text{host}}(\tilde{\nu}) \cdot \varepsilon_{\text{guest}}(\tilde{\nu}) \frac{d\tilde{\nu}}{\tilde{\nu}^4}, \tag{2}$$

where $F_{\text{host}}(\tilde{\nu})$ is the normalized spectral distribution of donor fluorescence, $\varepsilon_{\text{guest}}(\tilde{\nu})$ is the molar decadic extinction coefficient spectrum of the respective acceptor, and $\tilde{\nu}$ is the energy in wavenumbers. The overlap integral was similar for all studied blends (with $J_M=5.0\times10^{-11}$ cm^6/mol and $J_{G1}=J_{G2}=4.9\times10^{-11}$ cm^6/mol), yielding a Förster radius R_0 of about 29 Å. This value has to be compared to the minimum distance between the conjugated TPA-PF main chain and the core of the dendrimer. Lieser *et al.* showed that a comparable but slightly less bulky polyfluorene adopts a helical structure, with the main chains surrounded by the side chains and that the diameter of such a helix is in the range of 16 Å.[53] Molecular geometry optimization using the semiempirical PM3 method, as implemented in HYPERCHEM 5.1, yielded diameters of about 31 and 47 Å for G1 and G2, respectively.[17] The diameter of M was estimated to be 22 Å from the calculated increase in the molecular size dependent on the generation for the compounds shown in Chart 1.[23] Thus, the minimal possible center-to-center distances R between the transition dipole moments of donor and acceptor can be estimated to be approximately 19, 24, and 32 Å for M, G1, and G2, respectively. The fact that these values lie below R_0 for M and G1 explains the good energy transfer in these blends, whereas the larger distance results in a less pronounced transfer for G2. For an isolated donor-acceptor pair separated by a distance R_i, the Förster energy transfer rate $k_{\text{ET},i}$ is given by[51,52]

$$k_{\mathrm{ET},i} = \frac{9000 \ln 10}{128\pi^5} \frac{\kappa^2 \phi_{\mathrm{host}} J}{N_A n^4} \frac{1}{\tau R_i^6} = \frac{R_0^6}{\tau R_i^6}. \quad (3)$$

Here, τ is the donor fluorescence lifetime in the absence of the acceptor. The relation above is valid for the case of single donors and acceptors at a fixed distance, whereas in our films an excited donor can interact with a number of acceptor molecules. The total transfer energy is thus calculated by integrating over the film volume,[23,54]

$$k_{\mathrm{ET},i}^{\mathrm{tot}} = \int k_{\mathrm{ET},i} n_{\mathrm{guest}} dV = \frac{4\pi N_A \rho_{\mathrm{host}} c_{\mathrm{guest}}}{3\tau M_{\mathrm{guest}}} \frac{R_0^6}{(a+b_i)^3}, \quad (4)$$

where the number density of acceptor molecules n_{guest} is written in terms of the host density ρ_{host}, the weight concentration of guest molecules c_{guest}, and their molecular mass M_{guest}. The radii of guest and host molecules are a and b_i, respectively. The energy transfer efficiency $\eta_{\mathrm{ET},i}$ is given by

$$\eta_{\mathrm{ET},i} = \frac{k_{\mathrm{ET},i}^{\mathrm{tot}}}{k_{\mathrm{ET},i}^{\mathrm{tot}} + \frac{1}{\tau}} = \frac{1}{1 + \frac{3M_{\mathrm{guest}}}{4\pi N_A \rho_{\mathrm{host}} c_{\mathrm{guest}}} \frac{(a+b_i)^3}{R_0^6}}. \quad (5)$$

Assuming a mass density of 1 g/cm^3 for the matrix, the transfer efficiencies are $(83\pm6)\%$, $(53\pm10)\%$, and $(19\pm6)\%$ for M, G1, and G2, respectively. In other words, the transfer efficiency is predicted to drop to $(64\pm16)\%$ for G1 and to $(23\pm9)\%$ for G2 with respect to M. From the PL intensities shown in Fig. 2 (integrated above 550 nm), we calculate PL(G1)/PL(M)=66% and PL(G2)/PL(M)=10%. Considering the slightly decreasing fluorescence efficiency of the dendrimers with increasing generation due to the introduction of new nonradiative relaxation paths,[17,19] the calculated and measured values are quite in agreement. This supports our interpretation that the excitons generated on the TPA-PF chains are indeed transferred to the perylene dye via Förster energy transfer and that the TPA-PF chains do not penetrate the dendritic scaffold. It should be noted that our estimate does not take into account the migration of the exciton within the host.[55]

Charge-transport properties of the layers

In order to study the effect of doping on the charge-transport properties of the active blend layers, hole-only devices with 50 nm hole-injecting gold top electrodes were fabricated. Even though the position of the highest occupied molecular orbital (HOMO) level of TPA-PF with respect to the work function of ITO/PEDT:PSS or Au suggests that the current through such a sandwich structure is injection limited, investigations of these hole-only devices revealed a pronounced effect of the dopants on the current-voltage (I-V) characteristics (Fig. 4, open symbols). For voltages below 10 V, the current of the devices with the nondendronized M as dopant was almost one order of magnitude lower than for pure TPA-PF. The oxidation potential of M as determined from cyclic voltammetry (CV) in solution E_{ox}^0(M) is 1.0 V, which is 0.1 V lower than that of TPA-PF (E_{ox}^0(PF)=1.1 V versus Ag/AgCl). The decrease in the hole current indicates that the nondendronized M behaves as a shallow hole trap. Due to aggregation, the oxidation potential for M in films might be even smaller. For G1 and G2, the HOMO position matches that of PF, and the dye is not expected to trap holes [see Chart 4 for the HOMO and lowest unoccupied molecular orbital (LUMO) positions of all compounds]. According to this, doping either G1 or G2 into TPA-PF has no considerable effect on the I-V characteristics of hole-only devices.

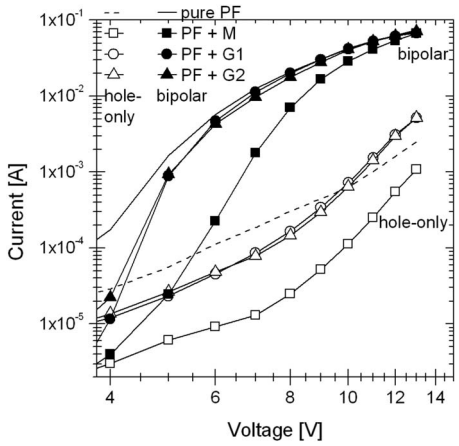

FIG. 4. Current-voltage characteristics of hole-only devices (open symbols) and the corresponding bipolar LED devices (filled symbols). Blends of TPA-PF with 3 wt % of M (squares), G1 (circles), and G2 (triangles) are compared with a pure TPA-PF device (no symbols). Due to fluctuations in the low voltage region, the results are plotted only for voltages higher than 3.5 V, for which the values were reproducible.

In comparison to the hole-only devices, a significant increase in current under forward bias was observed when electrons were injected from a LiF/Ca top electrode (Fig. 4, closed symbols). This confirms that electrons are the majority carriers in TPA-PF.[41,56] At low bias, the current through the bipolar devices dropped significantly upon doping. The comparison of the CV data for TPA-PF and for M, G1, and G2 suggests that all dyes behave as electron traps (the reduction peak potentials of the dopants, E_{red}^0(M)=−0.8 V, E_{red}^0(G1)=E_{red}^0(G2)=−1.0 V are considerably less negative compared to E_{red}^0 (PF=−1.9 V versus Ag/AgCl).[41] For higher voltages, the current of all the blend devices approached the values for those with pure TPA-PF, but for the model compound M this occurred only at remarkably higher voltages than in the case of the dendrimers G1 and G2. Noticeably, the current in both hole-only and bipolar devices does not depend on the generation for blends with Gl or G2. This indicates that the predominant fraction of charges is moving within the TPA-PF matrix, while few of them are captured on the PDI cores for generation 1 and 2 dendrimers.

Emission characteristics in electroluminescence

Figure 5 shows that the EL spectrum of nondendronized M in TPA-PF was dominated by the red emission from the

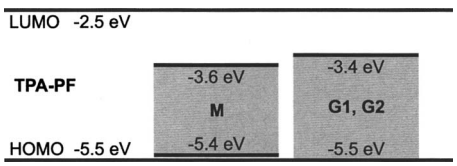

CHART 4. Energetic positions of the HOMO and LUMO levels for the different compounds calculated from CV reduction and oxidation potentials given in the text and assuming a reference potential of −4.4 V for Ag/AgCl.

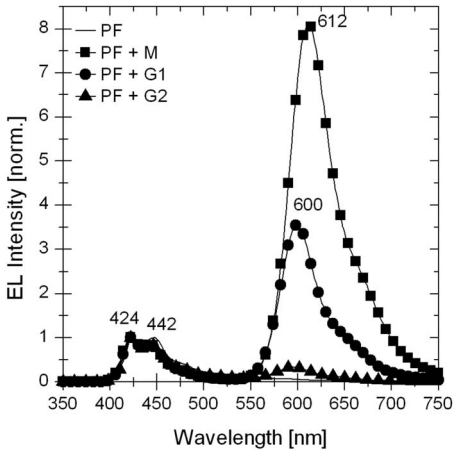

FIG. 5. EL spectra (normalized to the peak at 424 nm) for blends of TPA-PF with 3 wt % of M (squares), G1 (circles), and G2 (triangles). For comparison, the spectrum of the pure TPA-PF (solid line) is also shown. The spectra were recorded at a luminance of about 20 cd/m^2.

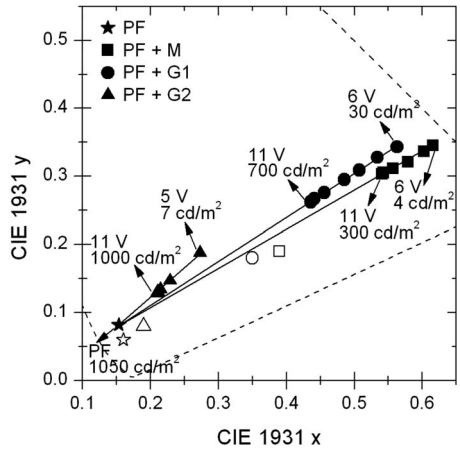

FIG. 6. Voltage dependent color change for LEDs of blends of TPA-PF with 3 wt % of M (squares), G1 (circles), and G2 (triangles), plotted in CIE 1931 coordinates (Ref. 48). The voltage independent value for a pure TPA-PF device is also shown (star). Open symbols depict the calculated color coordinates of the PL emission. The solid lines are guides to the eye; the dashed line denotes the edge of the CIE 1931 color space.

dye at 612 nm with a very weak contribution from TPA-PF at 421 nm. Predominant emission from the chromophore was still observed for the dendrimer G1 with the emission maximum at 600 nm. For the sample containing 3 wt % of G2, the EL spectrum was dominated by the host emission, and the relative intensity of the red emission was only one-third of that of the TPA-PF emission at 421 nm (at approximately 20 cd/m^2). A comparison of the EL spectra to the respective PL spectra shown in Fig. 2 shows that the emission from the PDI dye is generally much more pronounced in EL than it is in PL, indicating that a significant fraction of excitons is generated directly on the perylene dye rather than in the TPA-PF matrix. As discussed above, the chromophore sites are energetically more favorable for electrons than the TPA-PF sites. The resultant trapping of electrons increases the probability for hole capture and subsequent recombination on a chromophore.

Voltage dependent color changes

Figure 6 shows the dependence of the emissive color on the applied voltage for TPA-PF blended with 3 wt % of M, G1, and G2. For all samples the color coordinates changed to lower values, i.e., into the bluish region, when the driving voltage was increased. In all cases, the blueshift followed a straight line that, if extended, reaches the color coordinates of pure TPA-PF EL. Note that the PL color coordinates of the films display slightly lower ν values, which is mainly due to the difference between the PL and EL emission spectra of TPA-PF.

Emission properties and electron trapping

The effect of dendrimer generation on the emission color of the systems studied here was much more pronounced than reported previously for the blend of PVK:PBD with dendronized PDI. With increasing generation and increasing current density; the emission color changes from deep red to deep blue. The influence of the scaffold thickness on the EL properties is well seen when comparing the color coordinates of G1 and G2 devices. While the emission color of the G1 device was still reddish, with color coordinates (0.55, 0.35) at low bias, the corresponding G2 blend emitted bluish light with CIE coordinates (0.22, 0.18).

In our earlier publication we related the host and guest emission ratios in PL and EL, taking into account the kinetics of electron trapping by the emissive guest,[23]

$$\left.\frac{I_{\text{guest}}}{I_{\text{host}}}\right|_{\text{EL}} - \left.\frac{I_{\text{guest}}}{I_{\text{host}}}\right|_{\text{PL}} = \frac{\gamma}{\gamma_R}\frac{\phi_{\text{guest}}}{\phi_{\text{host}}}\frac{T_e}{p(1-\eta_{\text{ET},i})}. \tag{6}$$

Here, ϕ_{host} and ϕ_{guest} are the PL quantum yields of the host and the guest, respectively, $\eta_{\text{ET},i}$ is the efficiency of the Förster energy transfer of excitons formed on the host, γ is the electron-trapping coefficient, γ_R is the bimolecular recombination coefficient, T_e is the number density of the electron-trapping dye, and p is the density of mobile holes.

In order to quantify the effect of the scaffold on the trapping of charges by the PDI chromophore, we have calculated the ratio $I_{\text{guest}}/I_{\text{host}}|_{\text{EL}}$ from the CIE data shown in Fig. 6. Here we take advantage of the fact that the EL spectrum of the blend is a linear combination of the emission from the PF host and that of the pure dye. Therefore, the following approximation can be used:

$$\left.\frac{I_{\text{guest}}}{I_{\text{host}}}\right|_{\text{EL}} = \frac{x(\text{blend}) - x(\text{PF})}{x(\text{dye}) - x(\text{blend})}. \tag{7}$$

Here, x(blend), x(PF), and x(dye) are the CIE 1931 x-coordinates for the blend, the pure TPA-PF, and the pure dye, respectively. Values of $I_{\text{guest}}/I_{\text{host}}|_{\text{PL}}$ for all three blends have been calculated from the CIE coordinates of the respective PL spectra.

In Fig. 7, values for $I_{\text{guest}}/I_{\text{host}}|_{\text{EL}} - I_{\text{guest}}/I_{\text{host}}|_{\text{PL}}$, which can be considered to be a measure for the EL emission contribution caused by carrier trapping, are plotted as a function of bias. For all generations, we find a continuous decrease in the trapping contribution with increasing bias. This is expected since increasing the voltage will increase the number of mobile holes, and the direct recombination of electrons and holes on the TPA-PF backbone will become more likely.

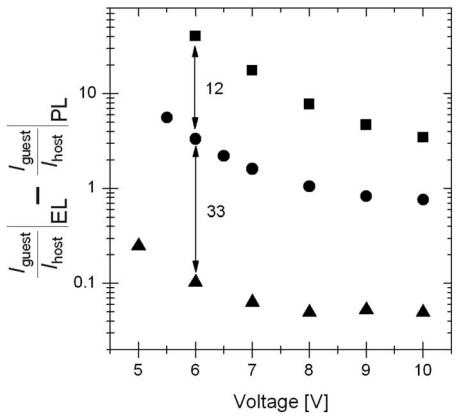

FIG. 7. Plot of $I_{guest}/I_{host}|_{EL} - I_{guest}/I_{host}|_{PL}$ as a function of voltage for TPA-PF with 3 wt % of M (squares), G1 (circles), and G2 (triangles). The ratios have been calculated, derived from the respective CIE *x*-coordinates using Eq. (7).

The field dependence of $I_{guest}/I_{host}|_{EL} - I_{guest}/I_{host}|_{PL}$ is quite comparable for all three blends, meaning that the underlying physical processes are almost the same. The main effect of increasing the dendrimer generation is thus a vertical offset of the curves, which we attribute mainly to a decreasing electron-trapping coefficient with increasing thickness of the dendritic scaffold.

A quantitative description of the voltage dependence of the trapping contribution to the EL emission would require exact knowledge of the hole density at a given voltage, the field dependence of the trapping and recombination efficiencies, and the extent of field-induced fluorescence quenching. These quantities are, unfortunately, not known to us. Since the voltage dependences of the current densities of the hole-only and bipolar devices made from blends with G1 and G2 are almost identical, we can presume that the charge carrier densities in both blends are similar. Using the values for the energy transfer efficiency $\eta_{ET,i}$ as given above and taking into account the different number densities of the dyes in blends with G1 and G2, the electron trapping coefficient γ is then calculated to decrease by a factor of about 8–10 upon adding one additional dendritic shell to G1. This is much larger than the effect of generation on electron trapping in the PVK:PBD:PDI system studied previously by us.[23] Large changes in the charge carrier properties and the OLED device properties with dendronization have been frequently observed.[57] For example, Lupton *et al.* measured the mobility of a family of dendrimers of generations 0–3. He found a significant decrease in mobility from approximately 10^{-6} cm^2 for the zeroth generation to about 10^{-8} cm^2/V s for the third generation (at moderate electric field).[18] A significant decrease in carrier mobility with generation was also reported by Markham *et al.* for highly fluorescent Ir-cored dendrimers.[58] In our system, the large change in the trapping coefficient with generation can be well understood from the fact that the polyfluorene backbone cannot penetrate the scaffold around the perylene dye. Therefore, the polyphenylene dendrons will act as an efficient barrier for electron trapping.

CONCLUSION

In conclusion, the emission properties of perylene dendrimers doped at small concentrations into a polyfluorene host are shown to be significantly affected by the thickness of the dendritic scaffold. In PL, the energy transfer of excitons from the TPA-PF host to the perylene core can be satisfactorily explained by Förster transfer through the isolating scaffold. In electroluminescence, the emission contribution from the perylene dye is significantly stronger than in photoluminescence but decreases with increasing bias. This is attributed to the competition between Förster energy transfer and electron trapping. For the model compound M and the first generation dendrimer G1, most excitons are generated directly on the perylene dye via charge carrier trapping, and the transfer of excitons generated on the TPA-PF host only gives a minor contribution to the perylene emission. For the second generation dendrimer G2, the thick scaffold effectively reduces the efficiency of electron trapping, and the EL emission of the blend approaches the PL spectrum for a high bias. From the comparison of the EL and PL spectra of both blends, we conclude that the coefficient for electron trapping is reduced by almost one order of magnitude from G1 to G2, significantly more than the reduction in the Förster transfer rate. This reduction is far more severe than in the blend of similar dyes with PVK:PBD.[23] As pointed out in the Introduction, the small molecule PBD might easily penetrate into the dendritic scaffold, providing a direct path for the electrons to the PDI core. Such interpenetration between the host and dendrimer seems quite unlikely in the present system.

On the other hand, the combination of dendronized dye molecules with small molecule charge-transporting moieties might be beneficial when seeking for the sufficient suppression of interactions between the emissive units and efficient transport of charges toward the dendritic cores. Various studies have shown that the addition of hole- and electron-transporting molecules to dendrimer-based active layers improves the device performance.[59–61] In this sense, dendrimers carrying charge-transporting moieties in the scaffold shall be very applicable for the realization of efficient molecular devices.[62]

For all blends, we observe a significant blueshift of the EL spectrum with bias. This is because electrons moving on the host can either be trapped on the guests or recombine with free holes. The latter process becomes more likely at higher hole concentrations, resulting in a smaller contribution by the guest emission. An increase in the relative guest emission intensity with increasing bias has been observed in the case of dye doped polymers or copolymers, for which the emissive guest functions as an electron trap.[10,12,63,64] We presume that these effects have a common origin, namely, the competition between the recombination of free electrons with free holes on the host and electron trappings (followed by recombination) by the emissive guest. We finally like to note that Gather *et al.* recently provided an alternative model to explain the color shift in a white-emitting copolymer comprising an electron-trapping red dye.[65] In this model, the emission color is determined by the competition between electron trapping on the red-emitting site and the unper-

turbed charge transport through the organic layer. A major drawback of the approach is that it essentially considers the kinetics of electrons in the active layer in the absence of holes. This is applicable only in cases where the hole density is very low. In general, the rate of recombination of free and trapped electrons with free holes needs to be taken into account when considering color shifts in multicomponent organic emission layers.

ACKNOWLEDGMENTS

We gratefully acknowledge Professor Dr. W. Knoll for the generous support and Dr. Vera Cimrova for fruitful discussions. We also thank Achmad Zen for recording the photoluminescence spectra. Financial support came from the European Commission (TMR Program SISITOMAS), SONY International (Europe) GmbH, and the Volkswagen Foundation.

[1] C. I. Chao and S. A. Chen, Appl. Phys. Lett. **73**, 426 (1998).
[2] A. R. Duggal, J. J. Shiang, C. M. Heller, and D. F. Foust, Appl. Phys. Lett. **80**, 3470 (2002).
[3] B. C. Krummacher, V. E. Choong, M. K. Mathai, S. A. Choulis, F. So, F. Jermann, T. Fiedler, and M. Zachau, Appl. Phys. Lett. **88**, 113506 (2006).
[4] Q. J. Sun, B. H. Fan, Z. A. Tan, C. H. Yang, Y. F. Li, and Y. Yang, Appl. Phys. Lett. **88**, 163510 (2006).
[5] M. C. Gather, A. Kohnen, A. Falcou, H. Becker, and K. Meerholz, Adv. Funct. Mater. **17**, 191 (2007).
[6] R. W. T. Higgins, A. P. Monkman, H. G. Nothofer, and U. Scherf, Appl. Phys. Lett. **79**, 857 (2001).
[7] Y. Kawamura, S. Yanagida, and S. R. Forrest, J. Appl. Phys. **92**, 87 (2002).
[8] X. Gong, W. L. Ma, J. C. Ostrowski, G. C. Bazan, D. Moses, and A. J. Heeger, Adv. Mater. (Weinheim, Ger.) **16**, 615 (2004).
[9] Y. H. Xu, J. B. Peng, Y. Q. Mo, Q. Hou, and Y. Cao, Appl. Phys. Lett. **86**, 163502 (2005).
[10] J. Liu, Q. Zhou, Y. Cheng, Y. Geng, L. Wang, D. Ma, X. Jing, and F. Wang, Adv. Mater. (Weinheim, Ger.) **17**, 2974 (2005).
[11] S. K. Lee, D. H. Hwang, B. J. Jung, N. S. Cho, J. D. Lee, and H. K. Shim, Adv. Funct. Mater. **15**, 1647 (2005).
[12] J. Jiang, Y. Xu, W. Yang, R. Guan, Z. Liu, H. Zhen, and Y. Cao, Adv. Mater. (Weinheim, Ger.) **18**, 1769 (2006).
[13] C. Y. Chuang, P. I. Shih, C. H. Chien, F. I. Wu, and C. F. Shu, Macromolecules **40**, 247 (2007).
[14] F.-I. Wu, X. H. Yang, D. Neher, R. Dodda, Y. H. Tseng, and C. F. Shu, Adv. Funct. Mater. **17**, 1085 (2007).
[15] M. Halim, J. N. G. Pillow, D. W. Samuel, and P. L. Burn, Adv. Mater. (Weinheim, Ger.) **11**, 371 (1999).
[16] S. Setayesh, A. C. Grimsdale, T. Weil, V. Enkelmann, K. Müllen, F. Meghdadi, E. J. W. List, and G. Leising, J. Am. Chem. Soc. **123**, 946 (2001).
[17] A. Herrmann, T. Weil, V. Sinigersky, U. M. Wiesler, T. Vosch, J. Hofkens, F. C. De Schryver, and K. Müllen, Chem.-Eur. J. **7**, 4844 (2001).
[18] J. M. Lupton, I. D. W. Samuel, R. Beavington, M. J. Frampton, P. L. Burn, and H. Bässler, Phys. Rev. B **63**, 155206 (2001).
[19] D. J. Liu, S. De Feyter, M. Cotlet, A. Stefan, U. M. Wiesler, A. Herrmann, D. Grebel-Koehler, J. Q. Qu, K. Müllen, and F. C. De Schryver, Macromolecules **36**, 5918 (2003).
[20] R. Beavington, M. J. Frampton, J. M. Lupton, P. L. Burn, and I. D. W. Samuel, Adv. Funct. Mater. **13**, 211 (2003).
[21] S.-C. Lo, T. D. Anthopoulos, E. B. Namdas, P. L. Burn, and I. D. W. Samuel, Adv. Mater. (Weinheim, Ger.) **17**, 1945 (2005).
[22] J. M. Lupton, in *Organic Light-Emitting Devices*, edited by K. Müllen and U. Scherf (Wiley-VCH, Weinheim, 2006), p. 265.
[23] J. Qu, J. Zhang, A. C. Grimsdale, K. Müllen, F. Jaiser, X. H. Yang, and D. Neher, Macromolecules **37**, 8297 (2004).
[24] A. Goetzberger and W. Greubel, Appl. Phys. **14**, 123 (1977).
[25] D. Schlettwein, D. Wöhrle, E. Karmann, and U. Melville, Chem. Mater. **6**, 3 (1994).
[26] M. P. O'Neil, M. P. Niemczyk, W. A. Svec, D. Gosztola, G. L. Gaines, and M. R. Wasielewski, Science **257**, 63 (1992).
[27] R. Gvishi, R. Reisfeld, and Z. Burshtein, Chem. Phys. Lett. **213**, 338 (1993).
[28] H. Murata, C. D. Merrit, H. Mattouossi, and Z. H. Kafafi (unpublished).
[29] J. Kalinowski, P. Di Marco, V. Fattori, L. Giulietti, and M. Cocchi, J. Appl. Phys. **83**, 4242 (1998).
[30] X. Z. Jiang, Y. Q. Liu, S. G. Liu, W. F. Qiu, X. Q. Song, and D. B. Zhu, Synth. Met. **91**, 253 (1997).
[31] H. Zollinger, *Color Chemistry* (VCH, Weinheim, 1987).
[32] X. Gong, M. R. Robinson, J. C. Ostrowski, D. Moses, G. C. Bazan, and A. J. Heeger, Adv. Mater. (Weinheim, Ger.) **14**, 581 (2002).
[33] X. H. Yang and D. Neher, Appl. Phys. Lett. **84**, 2476 (2004).
[34] X. H. Yang, D. Neher, D. Hertel, and T. K. Däubler, Adv. Mater. (Weinheim, Ger.) **16**, 161 (2004).
[35] X. H. Yang, D. C. Müller, D. Neher, and K. Meerholz, Adv. Mater. (Weinheim, Ger.) **18**, 948 (2006).
[36] R. A. Negres, X. Gong, J. C. Ostrowski, G. C. Bazan, D. Moses, and A. J. Heeger, Phys. Rev. B **68**, 115209 (2003).
[37] C. Y. Jiang, W. Yang, J. B. Peng, S. Xiao, and Y. Cao, Adv. Mater. (Weinheim, Ger.) **16**, 537 (2004).
[38] D. Neher, Macromol. Rapid Commun. **22**, 1366 (2001).
[39] U. Scherf and E. J. W. List, Adv. Mater. (Weinheim, Ger.) **14**, 477 (2002).
[40] A. W. Grice, D. D. C. Bradley, M. T. Bernius, M. Inbasekaran, W. W. Wu, and E. P. Woo, Appl. Phys. Lett. **73**, 629 (1998).
[41] T. Miteva, A. Meisel, W. Knoll, H. G. Nothofer, U. Scherf, D. C. Müller, K. Meerholz, A. Yasuda, and D. Neher, Adv. Mater. (Weinheim, Ger.) **13**, 565 (2001).
[42] T. Virgili, D. G. Lidzey, and D. D. C. Bradley, Adv. Mater. (Weinheim, Ger.) **12**, 58 (2000).
[43] P. A. Lane, L. C. Palilis, D. F. O'Brien, C. Giebeler, A. J. Cadby, D. G. Lidzey, A. J. Campbell, W. Blau, and D. D. C. Bradley, Phys. Rev. B **63**, 235206 (2001).
[44] F.-C. Chen, Y. Yang, M. E. Thompson, and J. Kido, Appl. Phys. Lett. **80**, 2308 (2002).
[45] H. A. Al Attar, A. P. Monkman, M. Tavasli, S. Bettington, and M. R. Bryce, Appl. Phys. Lett. **86**, 121101 (2005).
[46] X. Gong, S. Wang, D. Moses, G. C. Bazan, and A. J. Heeger, Adv. Mater. (Weinheim, Ger.) **17**, 2053 (2005).
[47] J. Huang, G. Li, E. Wu, Q. Xu, and Y. Yang, Adv. Mater. (Weinheim, Ger.) **18**, 114 (2006).
[48] Commission Internationale de l'Eclairage, http://www.cie.co.at, 2006.
[49] A. Stockman and L. T. Sharpe, CVRL Colour & Vision database, http://wwwcvrl.ucsd.edu/cmfs.htm, 2006.
[50] M. Pope and C. E. Swenberg, *Electronic Processes in Organic Crystals and Polymers*, 2nd ed. (Oxford University Press, New York, 1999).
[51] T. Förster, Ann. Phys. **2**, 55 (1948).
[52] T. Förster, Discuss. Faraday Soc. **27**, 7 (1959).
[53] G. Lieser, M. Oda, T. Miteva, A. Meisel, H. G. Nothofer, U. Scherf, and D. Neher, Macromolecules **33**, 4490 (2000).
[54] V. Bulovic, A. Shoustikov, M. A. Baldo, E. Bose, V. G. Kozlov, M. E. Thompson, and S. R. Forrest, Chem. Phys. Lett. **287**, 455 (1998).
[55] E. J. W. List, C. Creely, G. Leising, N. Schulte, A. D. Schlüter, U. Scherf, K. Müllen, and W. Graupner, Chem. Phys. Lett. **325**, 132 (2000).
[56] M. T. Bernius, M. Inbasekaran, J. O'Brien, and W. S. Wu, Adv. Mater. (Weinheim, Ger.) **12**, 1737 (2000).
[57] P. L. Burn, S. C. Lo, and I. D. W. Samuel, Adv. Mater. (Weinheim, Ger.) **19**, 1675 (2007).
[58] J. P. J. Markham, I. D. W. Samuel, S. C. Lo, P. L. Burn, M. Weiter, and H. Bässler, J. Appl. Phys. **95**, 438 (2004).
[59] J. P. J. Markham, S. C. Lo, S. W. Magennis, P. L. Burn, and I. D. W. Samuel, Appl. Phys. Lett. **80**, 2645 (2002).
[60] S. C. Lo, N. A. H. Male, J. P. J. Markham, S. W. Magennis, P. L. Burn, O. V. Salata, and I. D. W. Samuel, Adv. Mater. (Weinheim, Ger.) **14**, 975 (2002).
[61] T. D. Anthopoulos, J. P. J. Markham, E. B. Namdas, I. D. W. Samuel, S. C. Lo, and P. L. Burn, Appl. Phys. Lett. **82**, 4824 (2003).

[62] S. C. Lo, E. B. Namdas, C. P. Shipley, J. P. J. Markham, T. D. Anthopolous, P. L. Burn, and I. D. W. Samuel, Org. Electron. **7**, 85 (2006).
[63] J. Liu, S. Shao, L. Chen, Z. Xie, Y. Cheng, Y. Geng, L. Wang, X. Jing, and F. Wang, Adv. Mater. (Weinheim, Ger.) **19**, 1859 (2007).
[64] J. Liu, Z. Xie, Y. Cheng, Y. Geng, L. Wang, X. Jing, and F. Wang, Adv. Mater. (Weinheim, Ger.) **19**, 531 (2007).
[65] M. C. Gather, R. Alle, H. Becker, and K. Meerholz, Adv. Mater. (Weinheim, Ger.) **19**, 4460 (2007).